7

Modeling in Respiratory Movement Using LabVIEW and Simulink

Zhonghai He and Yuqian Zhao
Department of automation engineering, Northeastern University at Qinhuangdao
Qinhuangdao,
China

1. Introduction

The rapid pace of change in modern medicine makes training on simulation platforms an absolute necessity. With the microprocessors the sophistication of simulators exploded. More recently medicine has developed simulators that are becoming increasingly sophisticated, especially in anesthesia training but also to train intensive care personnel. This is an area that will rapidly advance in the future and will have great impact on medical education medical. Unfortunately, the current state of development for simulated procedural environments remains rather limited and the availability of validated metrics of skills acquisition is just beginning. There are two impulse to push respiration simulation forward, as list following.

1.1 Optimize mechanical ventilation

Mechanical ventilation is on the one hand the lifesaving therapy in intensive care medicine by all means. On the other hand this therapy can even aggravate the pulmonary status of the critically ill patient. Mechanical damage of the lung tissue is the predominant reason for ventilator induced lung injury (VILI). To avoid VILI, the physicians make great efforts to develop lung protective ventilation strategies (Grinnan, 2005). Lung protective ventilation considerably improves the outcome of mechanically ventilated and critically ill patients as it avoids extensive mechanical stress of the lung tissue and hence its irreversible damage. A valid analysis of respiratory mechanics is a prerequisite for lung protective ventilation. This analysis is always based on mathematical models. The equation of motion is the commonly accepted mathematical model of the respiratory system which provides the basis for the most clinically applied methods of respiratory mechanics analysis.

1.2 Medical patient simulator

Learning through hands-on experience is the best teaching method, but when reality is dangerous, events are rare and errors are costly, for instance in medical training, simulators are the preferred tools for teaching. The medical patient simulator (MPS) is one such tool used to train medical students and anesthesia residents. Sophisticated physiological and pharmacological mathematical models control mechanical actuator embedded in and adult-sized mannequin to create life-like physical signs and symptoms that health care personnel

use to make clinical diagnoses and to guide therapeutic interventions. As respiration is one of the most important physiology, the MPS has a self-regulating spontaneous breathing system that used pressurized gases in appropriate concentrations the enhance realism.

2. History of model construction

It has been long known that the mechanical properties of the airways and respiratory tissues exhibit different types of nonlinear behavior. In 1915 Rohrer suggested that the frictional pressure loss across the airways is a quadratic function of the volume flow rate. This Q dependence, originating from the nonlinear fluid mechanical aspects of gas flow in the airways, causes airway resistance to increase with increasing flow amplitude. Alternatively, in 1939, Bayliss and Robertson found that most of the viscous energy dissipated in the lung tissues during cyclic deformation did not depend on the flow rate but did depend on the amplitude of excursions, or tidal volume.

The first modern model as we know is described by Otis et al (1956) used to systematically examine the behavior of an inhomogeneous lung from a theoretical point of view. They assumed that the pressures to which the lungs are subjected are sine waves and inferred that time constant inequality could be responsible for the decrease in apparent compliance and resistance. Based on some reasonable approximations a single pulmonary pathway is regarded mechanically as consisting of a volume-elastic part having a compliance C, and a part having a resistance R, in series, which is the fundamental model of latter more complicated respiratory model. The success to this model is due to its simplicity, its immediate physiological interpretation, and its sensitivity to changes in lung mechanics.

The practical lung simulator is introduced by Clare E. Barkalow (1974, 1984). He invented a pneumatic lung analog for simulating spontaneous breathing and for testing of ventilatory devices used with spontaneously breathing patients and a kit for modifying training test lungs. The lung analog is comprised by mechanical parts and is the prototype of PneuView lung simulator of Michigan Instruments Inc.

The introduction of computers has made it possible to change quickly between different simulator settings. Meyer (1983) designed a microcomputer-controlled respiratory servo system, using a hydraulically operated cylinder-piston and solenoid valve assembly. The flexibility in selecting different breathing patterns allowed the implementation of complex sequences of breathing manoeuvers. Myojo (1989) described a breathing simulator with a split/cam valve without a piston/cylinder or bellows, the opening of the split/cam valve was controlled by a stepper motor under microcomputer control. This system allowed inspiratory flow patterns to be simulated as seen during spontaneous breathing, although it was not reported whether it was possible to change breathing patterns during simulation. Jansen (1989) described a computerized ventilator system for animal studies. Instead of the hydraulic system of Meyer, they used an electromechanical system, which was relatively small and easy to implement in the construction of a ventilator.

Verbraak adapted the idea of computer control and published series papers (1991, 1995, 2001, 2003) to drive a physical lung model for use in the pulmonary function laboratory to test lung function equipment. They use this computer-controlled mechanical lung model to perform pulmonary function tests on special breathing patterns in a body plethysmograph. The extended integration of hardware and software offers many new possibilities and advantages over the former simulators. The properties of components which simulate elastance and airway resistance of the lung are defined in software rather than by the

mechanical properties of the components alone. The lung model consists of three components: the actual lung model, an electromechanical servo system and a computer system to control the model.

Meka (2004) present a new bellow-less lung simulator utilizing a fixed-volume pressure controller to simulate spontaneous breathing as an alternative to the traditional bellows-driven mechanical lung system in the human patient simulator. The lung simulator simulates carinal pressure, which allows for simulation of actively breathing or ventilated patients. The bellow-less lung simulator drives up the precision of model because more action must be calculated by software.

It is well known that the large airway resistance is a nonlinear function of flow, and that total respiratory resistance depends on tidal volume, and is different on inspiration and expiration, being a continuous function of time during the respiratory cycle. It is a nonlinear phenomenon coupled with the airway collapse mechanism, seen as effort independence of flow for driving pressure exceeding a threshold value. Bernhard Quatember (2003) creates a mathematical nonlinear pressure-flow model with the following characteristic: avoid oversimplification model, airway partition by dynamic relationship, some mechanic parameters variation caused by pathology, and tries to model very precisely the tracheobronchial tree. However, there are still some points should be added in his model: first, airway collapse sometimes plays an important role; second, turbulent characteristic in large bronchi can not be neglected; third, more comprehensive pathology should be taken into account in modelling.

In 1998 Adam G. Polak (1998) has been constructed a complex, nonlinear forward model, including exciting signal and static recoil pressure lung volume descriptions and 132 parameters. In this case, the structural complexity is achieved at the expense of model linearization. It has been shown that lung heterogeneity plays an important role in respiratory system pathology and influences results of lung examinations. Experimental and model studies on the respiratory system demonstrate that heterogeneous constriction of airways accompany asthma and can be a crucial determinant of hyper-responsiveness via an increase in lung impedance.

In 2003 Adam G. Polak presented a computational model to predict maximal expiration through a morphometry-based asymmetrical bronchial tree. A computational model with the Horsfield-like geometry of the airway structure, including wave-speed flow limitation and taking into consideration separate airflows from several independent alveolar compartments has been derived. The airflow values are calculated for quasistatic conditions by solving a system of nonlinear differential equations describing static pressure losses along the airway branches. Then in 2006 he (Polak, 2006) use the nonlinear model to analyze the characteristic of lung mechanical ventilation.

In 2008 Adam G. Polak again investigated a model-based method for flow limitation analysis in the heterogeneous human lung. Flow limitation in the airways is a fundamental process constituting the maximal expiratory flow-volume curve. Its location is referred to as the choke point. In this work, expressions enabling the calculation of critical flows in the case of wave-speed, turbulent or viscous limitation were derived. Then a computational model for the forced expiration from the heterogeneous lung was used to analyse the regime and degree of flow limitation as well as movement and arrangement of the choke points. The conclusion is that flow limitation begins at similar time in every branch of the bronchial tree developing a parallel arrangement of the choke points.

3. Fluid dynamics theory used for respiratory model

3.1 Flow and resistance

Flow (Q) is the movement of air. Flow is dependent on a pressure gradient (Δp) and is inversely related to the resistance to flow (R). This relationship is described in the following equation: $Q = \Delta p / R$. In the lungs, two types of flow are present – laminar flow and turbulent flow. In general, turbulent flow is present in large airways and major bifurcations, whereas laminar flow is present in the more distant airways.

The steady flow is parabolic flow with radius and obtain Poiseuille theorem. In airways governed by laminar flow, resistance is related to the radius (r), airway length (l), and gas viscosity (η) through Poiseuille's Law ($R = 8\eta l / \pi r^4$). This equation highlights the strong relation of the radius on resistance. The turbulent flow shape is equal in center pipe and flow equation described by Rohrer's equation.

In a normal individual maximal inspiratory flow is limited only by muscle strength and total lung and chest wall compliance. Resistance to flow is minimal and does not limit inspiration. Maximal expiratory flow is initially limited only by expiratory muscle strength (when the airway radius is large and resistance is minimal). However, as the airway lumen decreases, resistance to flow will increase and flow is limited by resistance.

The wave speed theory of flow limitation is derived from fluid mechanics. When airflow approaches the speed of wave propagation within the airway wall, flow will be limited. According to this model, the cross-sectional area of the airway, the compliance of the airway and the resistance upstream from the flow limiting segment all contribute to flow limitation. This theory has been well validated during expiration, when vital capacity is between 0% and 75% of the total lung capacity. At a vital capacity greater than 75% of total lung capacity, it has been difficult to limit flow by increasing pleural pressure in normal individuals. Therefore, traditional teaching indicated that early expiration is primarily limited by effort dependent muscle strength. However, a recent model in normal individuals showed that peak expiratory flow was limited by mechanical properties of the lung (in accordance with the wave speed mechanism), and not by muscle strength (Tantucci, C., 2002). As peak flow normally occurs at around 80% of total lung capacity, the wave speed theory can be used to explain expiratory flow limitation from a vital capacity of 80% and less.

3.2 fluid theorems

A. Generalized Navier-Stokes equation

The basic equation of fluid dynamic is Navier-Stokes equation, as equation (1):

$$X - \frac{1}{\rho}\frac{\partial p}{\partial x} + \nu \nabla^2 u_x = \frac{du_x}{dt} \tag{1}$$

where p is pressure, u_x is velocity vector in x direction, x is body force, ρ is density, ν is kinetic viscosity.

B. Bernoulli energy equation

From classic fluid mechanics we obtain the following energy equation for a respiratory system in a closed loop pipe system with varying diameters

$$z + \frac{p}{\rho g} + \frac{u^2}{2g} = C \tag{2}$$

where z is spatial position, C is a constant value.

C. Conservation of mass

In steady flow, flow is continuous, mass conversation requires that

$$Q_{m1} = Q_{m2}, \quad Q_{m1} = \rho_1 Q_1 dt \tag{3}$$

Compliance with mass conservation law requires that flow rate in parent vessel must equal the total flow rate in children vessels on each branching level. Assuming that flow rate is constant for individual airway the continuity equation is expressed by

$$Q_0 = Q_1 + Q_2 \tag{4}$$

At a lung bifurcation the flow in the parent vessel Q_0 equals the sum of flow in two children segments Q_1 and Q_2 respectively.

D. Poiseuille theorem

Laminar flow is smooth, with molecules moving in parallel, concentric streams without eddies, and the molecules at the edge of the tube move more slowly than those in the middle. Laminar flow in Newtonian fluids (fluids with constant viscosities) is governed by Poiseuille's law. Poiseuille's law relates the air flow Q [ml/s] through airway with the difference in airway segment pressure at the two ends of vessel segment Δp created by the respiratory muscle, radius r, length L, and viscosity μ of the air:

$$R = \frac{8\mu L}{\pi r^4} \tag{5}$$

The resistance of air through vessels is most strongly dependent on radius, with the fourth power relationship. Because of fluid friction air flow velocity within vessel varies from none in wall proximity to maximum value in the center of the vessel creating parabolic velocity profile. Average velocity (with respect to cross-section) inside air vessel segment is determined as:

$$U_m = \frac{\Delta p * r^2}{8\mu * L} \tag{6}$$

E. Rohrer's equation

When flow rate through a tube reaches a critical velocity, turbulent flow occurs. In turbulent flow, the molecules swirl in eddies and vortices rather than in an orderly way, so that the molecules have a rotational as well as a linear velocity. Irregularities and corners in the tube facilitate turbulence. Conversion from laminar flow to turbulent flow approximately halves the flow for a given pressure drop.

If the flow is in high speed, the composition is altered, or if the internal part of the conduit is modified, the flow will become turbulent, and the equation to describe this phenomenon will be the following second–grad equation, as described by Rohrer (1915):

$$\Delta p = K_1 \times Q + K_2 \times Q^2 \tag{7}$$

where K_1 is the linear coefficient and K_2 is the angular coefficient of the straight line.

F. General pressure loss

The airflow values are calculated for quasistatic conditions by solving a system of nonlinear differential equations describing static result in the semi dynamic maximal expiratory flow-volume (MEFV) curve. This phenomenon has been described by Lambert et al. (1982) using the conservation of momentum (static, incompressible flow case):

$$\frac{dP}{dx} = \frac{-f(x)}{1 - S_{ws}^2(x)} = \frac{-f(x)}{1 - \frac{\rho q^2}{A^3(x)}\left(\frac{\partial A}{\partial P_{tm}}\right)} \tag{8}$$

Where dp/dx is the gradient of lateral pressure along the bronchus, $S_{ws} = u/c$ is the local speed index equal to the ratio between flow (u) and wave (c) speed, q is the volume flow in the bronchus, ρ denotes gas density, A is the cross sectional area, and $\partial A/\partial P_{tm}$ is the elementary compliance of the airway wall dependent on transmural pressure P_{tm}. The elementary dissipative pressure loss f (pressure drop per unit distance) is described by the following empirical formula (Renolds, D.B., 1982):

$$f(x) = \left(a + bR_N(x)\right)\frac{8\pi\mu q}{A^2(x)} \tag{9}$$

Where a and b are scaling coefficients, R_N the local Reynolds number and μ is gas viscosity.

4. Anatomical and physiology knowledge of airway and lung

4.1 Physiological characteristic

One of the most important problems in all the respiratory passageways is to keep them open to allow easy passage of the air to and from the alveoli. To keep the trachea from collapsing, multiple cartilage rings extend about five sixths of the way around the trachea. In the walls of the bronchi, less extensive cartilage plates also maintain a reasonable amount of rigidity yet allow sufficient motion for the lungs to expand and contract. These plates become progressively less extensive in the later generations of bronchi and are gone in the bronchioles, which usually have diameters less than 1.5mm (Guyton, 2002). The bronchioles are not prevented from collapsing by the rigidity of their walls. Instead, they are kept expanded by the same transpulmonary pressures that expand the alveoli. That is, as the alveoli enlarge, so do the bronchioles.

Under normal respiratory conditions, air flows through the respiratory passageways so easily that less than 1 cm of water pressure gradient from the alveoli to the atmosphere is sufficient to cause enough airflow for quiet breathing. The normal airway resistance of an adult is 0.1-0.3 kPa.s/L. The greatest amount of resistance to airflow occurs not in the minute air passages (diameter<1.5mm) of the terminal bronchioles but in some of the larger bronchi (diameter>1.5mm) near to the trachea, typically 80% in larger bronchi to 20% in minute passages in health physiology. The reason for this high resistance is that there are relatively few of these larger bronchi in comparison with about 65,000 parallel terminal bronchioles, through each of which only a minute amount of air must pass. Yet in disease conditions, the smaller bronchioles often do play a far greater role in determining airflow resistance, for two reasons: (1) because of their small size, they are easily occluded; and (2) because they have a greater percentage of smooth muscle in the walls, they constrict easily.

4.2 Morphometric model of the lung and the corresponding fluid dynamic

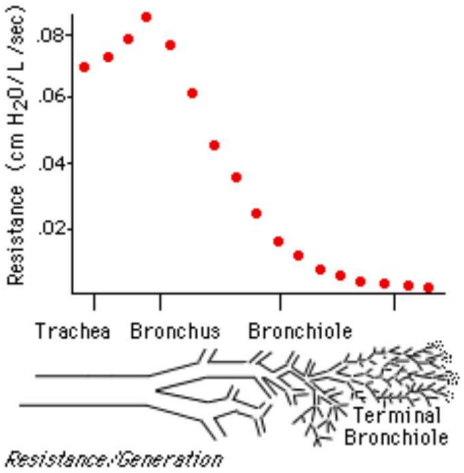

Fig. 1. Typical airway resistance value for every generation

1	2	3	4	5	6	7	8
0.0701	0.0732	0.0788	0.0856	0.0769	0.0620	0.0459	0.0360
9	10	11	12	13	14	15	16
0.0248	0.0161	0.0118	0.0074	0.0056	0.0037	0.0031	0.0025
17							
0.0019							

Table 1. Resistance for passage airway, same value with Fig. 1

The morphometric model used to describe the behavior of the respiratory system is based on the symmetrical model proposed by Weibel (1963). In this model the tracheobronchial tree is divided into 24 generations, where generation 0 is the trachea, generation 1 is extrapulmonary bronchus, generations 2 to 6 are larger intrapulmonary bronchi with cartilage, generations 7 to 16 are bronchioles with smooth muscle, generations 17 to 22 are all respiratory bronchioles, and generation 23 corresponds to alveolar sacs. The airways multiply by regular dichotomy. Starting from the trachea, each branch of a given generation divides into two identical daughters, therefore generation n has 2^n branches. In a spontaneous breathing, normal person, the medium-sized bronchi are the site of greatest resistance (Ball, Wilmot C., 1996), see the data (table 1) and graph (figure 1) of airway resistance.

4.3 Collapsible tube model and flow limitation

Limitation of flow is caused by airway wall collapsing, which follows the drop of transmural pressure (i.e. the difference between internal lateral and external pressure) along a bronchus. There are a few mechanisms influencing the decrease of transmural pressure in quasi-static conditions. The first of them is the loss of pressure due to frictional and turbulent dissipation of gas energy. It entails the drop of internal pressure and then narrowing of an elastic airway. This change in the cross-sectional area of the bronchus forces increase of gas velocity, thus enlargement of the kinetic component of gas energy. This

convective acceleration absorbs a part of potential energy (thus also of lateral pressure), producing additional decrease of transmural pressure. It was theoretically discussed and shown that these two processes can produce flow limitation themselves. Additionally, when flow velocity approaches wave-speed of pressure disturbance propagation along the airway wall, the loss of lateral pressure is strongly amplified, and the airway narrows much quicker than in case of frictional or turbulent dissipation alone. In effect, increasing driving pressure tries to develop faster airflow, but any growth of flow would have produced faster airway collapsing, overcoming the expansion of pressure, and finally, flow remains constant. The wave-speed theory predicts flow over most of vital capacity (V_C, the maximal volume of air that can be expired after deep inspiration), but the other mechanisms may limit flow at low lung volumes.

The wave velocity in fluid-filled collapsible tube is the following equation:

$$c = \left(\frac{A}{\rho} \frac{dp}{dA} \right)^{1/2} \tag{10}$$

where A is the mean cross-sectional area of the tube, p is the transmural pressure in the tube (the inner minus the outer pressure), and ρ the fluid density. The equation crops up in the study of wave propagation in pulmonary passages.

The principal characteristic of pliable, collapsible tubes is that, as the pressure therein changes, so does the cross sectional area. Similarity of Eq. (10) to that for propagation of waves in a compressible gas is evident once it is realized that such waves involve variations in density rather than the cross-sectional area; so, if A is replaced by r, this results in

$$c = \left(dp/d\rho \right)^{1/2}$$

An interesting phenomenon arising in collapsible tubes with internal flow is that of flow limitation. As the upstream pressure p_1 is increased relative to the downstream one p_2, thus as $p_{1-2} = p_1 - p_2$ is increased, there exists a limit in the flow-rate Q; if p_{1-2} is increased further, no further increase in Q is possible. This, obviously, is very counter-intuitive from the point of view of rigid-pipe hydraulics.

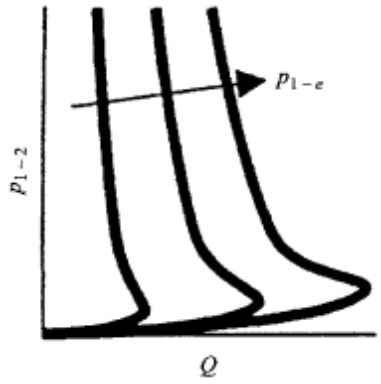

Fig. 2. The relationship between the upstream-to-downstream pressure difference p_{1-2} in a collapsible tube conveying fluid

As seen in Fig. 2, obtained from experimental measurements by Bertram (1995), for a constant transmural pressure at the upstream end of the tube, denoted by p_{1-e} (e standing for external), and varying p_{2-e}, as p_{1-2} increases there is a limit for Q, a maximum value; three such cases are shown in the figure for three different values of p_{1-e}. In fact, the flow rate decreases somewhat with increasing p_{1-2} beyond that yielding the maximum Q. This corresponds to the so-called "negative effort dependency" in maximal flow expiration. In an appealing analogy, flow limitation is likened to flow over a waterfall, where the flow-rate is independent of the level of the downstream reservoir. One of the mechanisms associated with flow limitation in collapsible tubes is the so-called wave-speed mechanism, with strong analogy to gas dynamics. One may calculate

$$\frac{dQ}{dp} = \frac{A}{\rho U}\left(1 - \frac{U^2}{c^2}\right) \tag{11}$$

where Q is the volumetric flow-rate in the collapsible tube, p the transmural pressure, A the cross-sectional area, U the flow velocity corresponding to any particular A (both A and U vary along the tube), and c the wave speed as in Eq. (10).
It is obvious that as

$$\frac{U}{c} \to 1$$

There is a discontinuity associated with a maximum flow rate in the collapsible tube. This is also associated with so-called elastic jumps. Thus, in all this, the analogy to choked flow and shock waves in gas dynamics is quite strong.

4.4 Airway segment based on different fluid dynamic performance

Based on anatomical structure the entire respiratory system (including airway and lung) can be divided into two zones: conductive zone (generation 0 to 16) and respiratory zone (generation 17 to 23). In conductive zone the airway resistance is the main effective factor. At the same time in respiratory zone the compliance is the dominant parameter. The last 7 generations (respiratory zone) are modeled as a single viscoelastic element with constant values; chest wall is combined in lung compliance value.

A. Thoracic cage and respiratory muscles

The lung and airways were assumed to be enclosed within a rigid-walled thoracic cage, with the airways open to the atmosphere. The intrapleural space was assumed to be subject to a time-varying, spatially averaged driving intrapleural pressure [$P_{p\ 1}(t)$], which was assumed to be equivalent to the average pressure in the pleural space acting on the lungs and produced by the muscles of respiration. Excursion in P_{pl} was dictated by the effort generated by the subject.

B. Alveolar region

Alveolar region (of volume V_A) was assumed to exhibit nonlinear, time-varying viscoelastic behavior. Static elastic behavior of the lung (P_{el}*vs.*V_A) was described by a hysteretic pressure-volume (P-V) relationship. The extent of hysteresis in P_{el} was presumed to be a function of breathing effort, which, in turn, was assumed to be proportional to P_{pl} (reflecting muscular effort). Hence, the dependence of P_{el} on P_{pl} served to define the well-known

hysteretic path. Viscous dissipative characteristics exhibited by lung tissue were characterized by using a constant lung tissue resistance R_L.

C. Peripheral airways

Peripheral airways were characterized by a resistance (R_s) that was inversely proportional to V_A. Airway closure during forced expiration causes occlusion of these airways at low alveolar volumes. Because of the effect of large intrathoracic pressures generated during the effort-dependent portion of forced expiration, R_s was modified to be a function of both V_A and P_{pl}.

D. Collapsible airways region

Collapsible airway region (of volume V_c) was characterized in terms of a volume-dependent resistance and a volume-pressure relationship $(V_C - P_{tm})$. The functional importance of this collapsible segment has since been confirmed by analyze the input impedance spectrum vs. frequency and demonstrated that adequate reconstruction of pressure-flow data could not be achieved with a conventional single-compartment resistive-compliant model. Previous studies have demonstrated that in lumped models expiratory flow limitation during the FVC maneuver cannot be simulated without the presence of this collapsible segment. Verbraak et al. (1991) modeled the elastic properties of the compressible segment as a family of curves dependent on the lung elastic recoil. This more complex approach proved to be of little benefit in achieving good fits to subject data.

E. Upper airway region

Upper airway region (of volume V_D) was assumed to be rigid, with its resistance to airflow characterized by a nonlinear, flow-dependent Rohrer resistor.

Summarized from fluid dynamic analysis the conductive zone can be segmented into two parts, i.e., the larger airway and the small airway, which have different flow behaviors. For lung simulator aim we segment the airway by fluid dynamic performance of different generations. Existed analysis (Polak, 2006) reveals three sections of the bronchial tree with distinct resistive properties. Generations 0–6 are characterized mainly by turbulent dissipation of the head pressure, laminar flow and airways collapsing dominate in generations from 7 to 16 (Mauroy, 2004), and lastly, flow in generations from 17 to 23 is approximately laminar, where compliance, not resistance, is the main parameter.

4.5 Different pathology and segments they influenced

The respiratory ventilation functional obstruction can be divided into two main types: restrictive hypoventilation and obstructive hypoventilation. The restrictive hypoventilation is mainly cause by two factors: respiratory muscle activation decrease and compliance decrease of lung. The disease such as fibrosis, pneumothorax, pulmonary overventilation, lung edema, can cause compliance decrease. In simulation model, the muscle decrease can be simulated by muscle driven pressure, and the aforementioned lung diseases have influence on lung compliance. The obstructive hypoventilation is mainly caused by airway stricture or obstacle. The disease typically emphysematous, asthmatic lung and larger airway occluded are obstructive.

The obstructive hypoventilation can also be divided into two types: central airway obstacle and peripheral airway obstacle. The central airway obstacle can further divided into extrapleural and intrapleural obstacle. The extrapleural obstacle locate in trachea and main bronchi which extrapleural, correspond to generations 0 and 1. The extrapleural obstacle shows inspiration difficult. The intrapleural central airway obstacle locate in bronchi

intrapleural and is expiration difficult. To show this different localization obstacle, we must subdivide the upper airway into two segments: the extrapleural segment and intrapleural segment which have different symptom in respiratory disorders.
For the purpose of modeling, the pulmonary system has to be simplified to elements which represent specific physical features of the lung. The lung model was restricted to serial inhomogeneity with respect to both resistance and elastic properties of the airways. The currently prepared mathematical model is based on serial model consists of one alveolar compartment connected to ambient air by a tube representing the airways. All alveoli were lumped to one compartment V_A, which was connected to ambient air by a tube representing the lumped airways. This tube consisted of four parts in series: one for the small airways, a compressible segment in between, one for the large airways intrapleural, and the last one for large airways extrapleural. The alveolar compartment and the intrapulmonary airways were influenced by the intrathoracic pressure, which was equal to pleural pressure P_{pl}. In preliminary result, the serial model of lung can be schemed in figure 3.

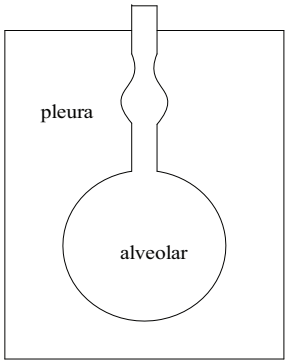

Fig. 3. Serial lung model with airway segment

5. Respiratory model with different complication

5.1 Simple linear model

There are many models describe breathing movement with different complication. It is possible to construct a model with a single volume-elastic unit and a single flow-resistance unit (e.g. a rubber bellows connected to a glass tube) which conforms mechanically to simple linear model.
The simplest and fundamental model consisting of a volume-elastic part having a compliance C and a resistance R in series. These equations are analogous to equations which define electrical capacitance and electrical resistance, respectively. If the total pressure across the system at any moment is Δp , then

$$\Delta p = \frac{1}{C} V + RQ \tag{12}$$

Since the compliance and resistance of a single pathway are constants, the total pressure will be determined at any instant by the volume of the unit and the rate and direction of flow at that instant.

Recent studies have shown that this first-order model is, however, an oversimplified representation of nonlinear, multicompartment respiratory mechanics. In fact, it is well known that the large airway resistance is a nonlinear function of flow, and that total respiratory resistance depends on tidal volume, and is different on inspiration and expiration, being a continuous function of time during the respiratory cycle. Parameter estimates based on the first-order model, therefore, do not depend solely on patient condition but also on experimental condition, because the model involves linearization around the working point.

5.2 Complicated compliance nonlinear model

The numerically simulated model features a two component resistance, representing the series association of a linear resistor with a flow-dependent resistor. The latter models nonlinear tracheal tube characteristics, and the former lumps the linear part of the tracheal tube resistance together with the equivalent linear resistor of the respiratory system. The model of elastance was proposed with a volume-independent and a volume-dependent component. The equation of motion that represents this model is:

$$P_{aw} = \left(K_1 + K_2\left|Q(t)\right|\right)Q(t) + \left(E_1 + E_2 V(t)\right)V(t) + P_0 \tag{13}$$

where Paw(t) is the pressure measured at the airway opening at time t, Q(t) the flow, V(t) the volume and P0the constant.

The basic model values used in this work ($E_1 = 50 cmH_2OL^{-1}$, $E_2 = -80 cmH_2OL^{-2}$, $K_1 = 10 cmH_2OL^{-1}s$, $K_2 = 5 cmH_2OL^{-2}s^2$) lie within the range observed in data obtained from animal experiments described elsewhere (Jandre et al., 2004). The negative E_2 suggests alveolar recruitment throughout the respiratory cycle.

5.3 Nonlinear simulation model of breathing mechanics with airway segment

In this model, the viscoelastic properties of the tracheobronchial airways are characterized by nonlinear relationships, whereas the behavior of the alveolar space and chest wall are assumed to be linear. The airway behavior is described by a physiological representation, incorporating a mechanism causing expiratory flow limitation, which has proved useful for the clinical interpretation of lung function tests and for describing the dependence of total respiratory resistance on frequency and tidal volume, in line with experimental evidence. Airway resistance was divided into the following three components:

1. upper airway resistance, R_u, modeled by a nonlinear Rohrer resistor depending on flow:

$$R_u = K_1 + K_2\left|Q\right| \tag{14}$$

   where the constant K_1 represents resistive properties for laminar flow, and the constant K_2characterizes an additional resistive term, significant at higher flow rates when turbulence may occur;

2. intermediate airway resistance R_i, depending on the airway compression due to transmural pressure. This segment was modeled as a cylinder of constant length, the radius and hence volume (v_c) of which vary with transmural pressure. On the basis of Poiseuille's law, the corresponding resistance is described by

$$R_i = K_3\left(\frac{v_{c\max}}{v_c}\right)^2 \tag{15}$$

where the constant K_3 represents the value of R_i when airway volume reaches its maximum admissible value v_{cmax}; and

3. lower airway resistance R_i , depending on lung volume (v). Since R_i decreases with increasing lung volume, it was described by the following relationship:

$$R_l = \frac{K_4}{v} \tag{16}$$

Where K_4 is a positive constant.

On the basis of experimental data the elastic characteristic of the intermediate airway segment is approximated by the relationship:

$$\frac{v_c}{v_{c\max}} = \frac{1}{1+\exp\left[-a\left(p_{tm}-b\right)\right]} \tag{17}$$

where a and b are constants and P_{tm} is the transmural pressure. Differentiating v_c with respect to p_{tm} , we obtain the intermediate airway compliance C_{aw} .

Finally, since this chapter is aimed at establishing respiratory model have the nonlinear mechanical properties of the tracheobronchial airways, the alveolar space and chest wall were assumed to have a constant, purely elastic behavior and were represented by the constant elastance respectively.

6. Simulation method

6.1 General description

LabVIEW and Matlab are the two main programs used widely by engineer. LabVIEW is a well opened virtual instruments platform and widely used in automatic control and measuring technology. LabVIEW simplify development procedure of process control and testing software. Now, LabVIEW has become the main trend of measuring and testing technologies and instruments. With the strong hardware interface capability, LabVIEW can communicate with other hardware and acquire data easily. But LabVIEW has limited toolboxes which confine the using field to large application program, in the case of complex applications having large data processing and complicate control algorithm, LabVIEW is not competent. Conversely, Matlab has very strong computing functions and stable algorithm library. Matlab provides precision and high efficiency toolboxes in almost all engineering computing fields. But it is not proficiency for interface compile. And data input, net communication, hardware control are also shortcoming of matlab. Because the two languages have complimentary specialties, we can combine the advantage by mixture programming. The data collected by LabVIEW can be sending to matlab for computing, and then processed data transfer back to LabVIEW for output control and display. Calling matlab in LabVIEW can control hardware easily and realize complex algorithm concurrently.

The Simulation Interface Toolkit provides methods for creating a LabVIEW user interface for a Simulink model, converting a Simulink model into a dynamic link library (DLL), and running a simulation model on an RT target. By combining the capabilities of Simulink and Real-Time Workshop with LabVIEW, the Simulation Interface Toolkit helps you import simulation models into LabVIEW.

6.2 Simplest model simulation

There are two distinct approaches to generating the simulated respiratory movement. The first is a simulation script and another one is model-driven simulation. The state-of-the-art medical patient simulator is physiological model driven simulator, so generating suitable physiological signal is the key task of medical patient simulator.

In order to describe the spontaneous respiratory model fundamentality in a simple and direct way, the following principles are adopted: structure of respiratory system is described by the simplest model, i.e., only lung compliance (C) and airway resistance (R) are taken into consideration; respiratory muscle pressure is used as input of model. With the above hypothesis, the constructed model can reflect the basic characteristic in general.

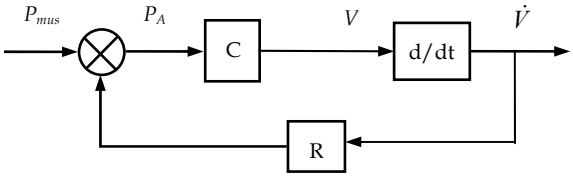

Fig. 4. Respiratory model based on muscle pressure driven

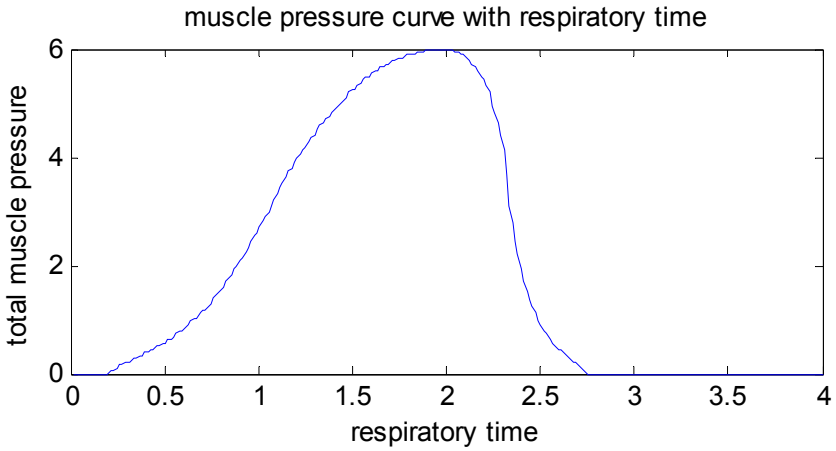

Fig. 5. Pressure waveform generated by respiratory muscle

The simplest mathematical model of respiratory system is linear model:

$$P_{mus} = \frac{1}{C}V(t) + R\dot{V}(t) \tag{12}$$

Which P_{mus} is respiratory pressure, generated by respiratory muscle, C is compliance, R is airway resistance, $V(t)$ is air volume breathed in lung, $\dot{V}(t)$ is air flow of respiratory, being the derivative of volume to time. In the model the compressibility of air is neglected as usual. There are two basic parameters in describing the respiratory system: compliance C and airway resistance R. Based on the linear model described above, the simplest respiratory model we established is shown in figure 4. The merits of the model are listed on

the following: (1) simple model, most details are neglected; (2) from distinct principle, spontaneous respiratory can be concluded from the model; (3) extensive expansibility, every component can be complicated if needed, so that complexity of model's study can be selected as requirement.

The parameters of R and C in model can be selected as normal human; while the respiratory muscle pressure can be acquired precisely from the data of Jodat et al.(1966) image processing, as shown in figure 5. In Simulink the muscle pressure used as input, the breath mechanical parameters (*R* and *C*) is the linear response system, then the spontaneous respiratory waveform can be computed.

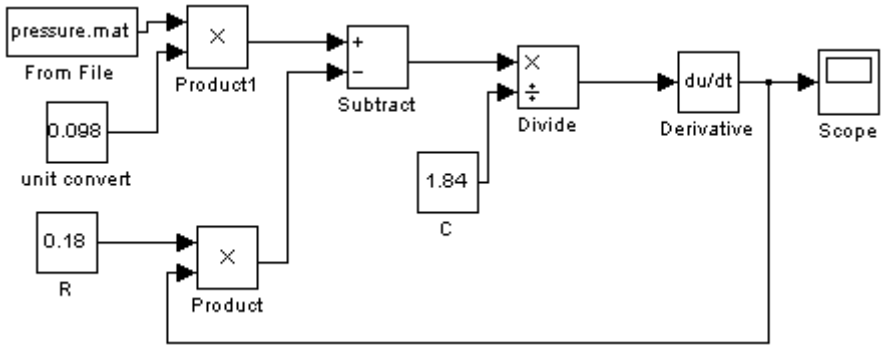

Fig. 6. Spontaneous respiratory model simulated by Simulink

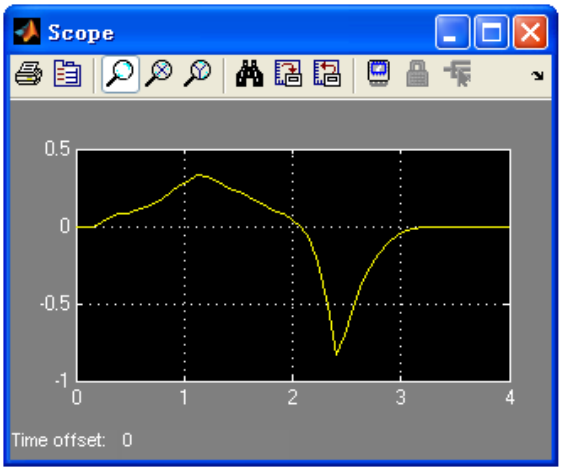

Fig. 7. Respiratory flow waveform by muscle pressure driven using Simulink

Typical parameters of human respiratory system is used in simulation, parameters being R=0.18kPa.s/L, C=1.84L/kPa (Tang, 1995). Particular Simulink model is shown in figure 6, and the simulation result shown in figure 7.

Compared with the respiratory flow given in reference (Bachy, 1986), it can be concluded that the two flow waves are very similar. They both have smooth inspiratory flow wave and

rather sharp expiratory flow wave, but have the same volume in the two breath phase. The expiratory flow is originate from the relax of breath muscle, together with the delay of respiratory system to airflow. The two main facts make the expiratory flow being a sharp flow at the beginning and then a long time without airflow. Change the parameters of respiratory system, the shape of flow variate, and so is the frequency spectrum of flow waveform, which is in accordance with Benchetrit's (2000) conclusion. Because respiratory pressure waveform is not single frequency sine wave, change the pressure waveform will change the frequency spectrum of respiratory flow wave too, so pressure waveform generated by respiratory muscle is an influence factor to flow frequency spectrum. The frequency of the breath system can also be changed by variation of the mechanical parameters, which is similar to one-order RC circuit. The linear system can not create the non-existing frequency, however, the input (muscle pressure) of the linear system (breath system) the muscle pressure contain abundant frequency, as a result the output (airflow) also include harmonic frequency. Once the input and mechanical parameters do not change abruptly, the output will remain a suitable stable frequency content.

6.3 Adjustable respiratory mechanical parameters lung system

In our simulation, all mechanical parameters of the lungs (pressure, compliance, resistance, volume) can be reduced to airflow, which is the most important variable to be measured in clinical. We design a new approach to simulate the lung system, which has the following characteristics. First, the basic hardware structure of the lung is similar to Meka's (2004). Second, breath flow is tracked in stead of carinal pressure, which is the most important parameter in respiration and calculated by respiratory model. Third, the resistance and compliance are adjustable in the simulation model. The influence of the two facts, i.e., compliance (C) and resistance (R), to the breath can be observed distinctly in our model. Four, the entire system is small size as the advantage of bellows-less lung simulator.

Current simulator models the flow in and out the lung to simulate physically character of respiratory system. We design the lung simulator based on the breath principle. This paper construct normal human respiratory system model, combined the widely used respiratory model and muscle pressure driven power. Then the breath flow wave is tracked by proportional valve controlled by calculated output voltage.

There are two main methods for simulation that are widely used, one is Simulink in matlab, and another is control design and simulation module in LabVIEW. Compared with matlab, LabVIEW not only easy to realize parameter collection and control parameter output, but also convenient to realize in hardware. As to Simulink in matlab, after the realization on algorithm, it is usually needed to transform to C language in order to combine with hardware, compile language is necessary sometimes. We have done the simulation in Simulink (He, 2009(a)), and we met the foregoing difficulty, i.e., how to realize the algorithm on hardware. In this chapter, we give the simulation method based on LabVIEW. Because of different simulation way between the two programs, different models are used base on same principle.

Not similar to the Simulink model, the convenient way to construct the respiratory model in Control Design and Simulation module in LabVIEW is to use linear system theory. An electro-acoustic analogy (Ma, 1983) is used to develop an electric model of the respiratory system in despite of its exact anatomical structure. In order to describe the spontaneous respiratory model fundamentality in a simple and direct way, the following principles are

adopted: structure of respiratory system is described by the simplest model, i.e., only lung compliance (C) and airway resistance (R) are taken into consideration; respiratory muscle pressure data is used as input of model into the linear system; transfer function is generated by first-order RC circuits. With the above hypothesis, the constructed model can reflect the basic characteristic in general. Then the output is calculated by linear system theory and realized in LabVIEW by CD linear simulation.vi located in Control Design and Simulation module. The final output represents the volume variation of every breath. After differentiate the volume, respiratory flow is gained that can be traced by hardware.
The simplest mathematical model of respiratory system is linear model (Otis, 1956):

$$P_{mus} = \frac{1}{C}V(t) + R\dot{V}(t) \tag{12}$$

Then the transfer function of volume of compliance can be calculated as

$$F(S) = \frac{1}{RCS+1} \tag{18}$$

Which P_{mus} is respiratory pressure, generated by respiratory muscle, C is compliance, R is airway resistance, V(t) is air volume breathed in lung, $\dot{V}(t)$ is air flow of respiratory, being the derivative of volume to time. In the model the compressibility of air is neglected as usual.
Typical parameters of human respiratory system is used in simulation, parameters being R=0.18kPa.s/L, C=1.84L/kPa (Tang, 1995). The related LabVIEW program is shown in figure 8, and the simulation result shown in figure 9.
Compared with the respiratory flow given in (Bachy, 1986), it can be concluded that the two flow waves are very similar. Change the parameters of respiratory system, the shape of flow change, and so is the frequency spectrum of flow waveform, which is in accordance with Benchetrit's (2000) conclusion. Because respiratory pressure waveform is not simple sine wave, changing the pressure waveform will change the frequency spectrum of respiratory flow wave too, so pressure waveform generated by respiratory muscle is an influence factor to flow frequency spectrum.

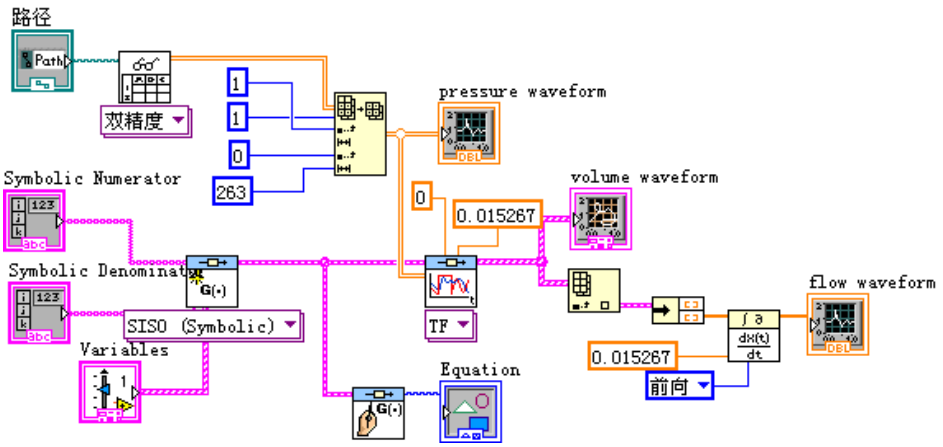

Fig. 8. Block diagram of respiratory simulation using transfer

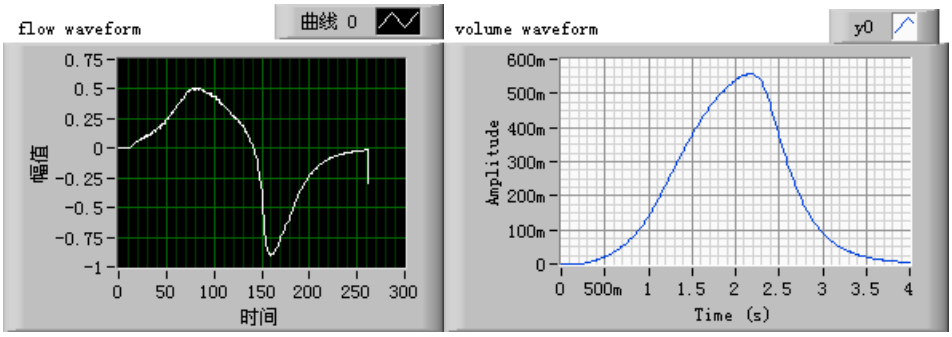

(a) (b)

Fig. 9. The simulation results calculated by transfer function of the respiratory
(a) flow waveform of one breath cycle (b) volume curve of one breath cycle

We used a fixed volume flow controller to generate the required airway flow. The flow controller is based on the ideal gas law. Air compression is neglected in this model, which is common practice. Flow is generated inside a fixed volume at a constant temperature by adjustment of the orifice of proportional valves. In flow is generated when gas is pumped into the fixed volume, and likewise out flow is generated when gas is removed from the volume. The airway resistor was constructed in the direction of Mecklenburgh (1988). The flow system consists of a fixed-volume vessel (FVV), a positive pressure source, a negative pressure source, two proportional flow valves (PFV), a flow sensor, a computer with data acquisition card. The entire setup is illustrated in Fig.10. The two pressure sources are implemented by air pump and vacuum respectively.

The fixed-volume vessel is a cylindrical-shaped polyvinyl chloride (PVC) structure. The cylindrical shape reduces turbulent gas flow inside the container, and the PVC material allows for inexpensive, quick and easy assembly of the structure. The vessel has three openings to allow the flow of gas in and out of the FVV to simulate ventilation. The outlet also facilitates the fitting of standard clinical airway resistors. The vessel is sealed airtight using PVC cement to prevent any air leaks from the container.

The volume of the FVV was determined experimentally by measuring the flow rate for various vessel volumes. The size of the volume was chosen to balance time delay and controllability. Time delay increases for larger vessels, because the vessel needs to fill completely before the flow starts to rise. Controllability is affected mainly by the volume of the vessel. It is easier to control the flow in a larger vessel, because compressibility of gas increases the total vessel compliance. It is difficult to control the flow in a very stiff vessel, because a small addition of volume increases the flow rapidly. With the available materials, a volume of 0.64 l was realized.

Two proportional flow control valves (IQ valves co., P/N: 209090) were used for control flow in and out of FVV. Pulse width modulated (PWM) solenoid valve drivers (Burr-Brown Company, DRV101) were used to run the proportional flow valves. An added advantage of the PWM waveform was that it reduced valve magnetic hysteresis and minimized power loss and component overheating at high current levels. The duty cycle of the pulse width determined the amount of power delivered to the valve. A 16-bit DAQ card (NI, PCI-6221M, with 16 analog inputs and 2 analog outputs, all in 16-bits resolution) supplied the signal to adjust the duty cycle of the pulse width.

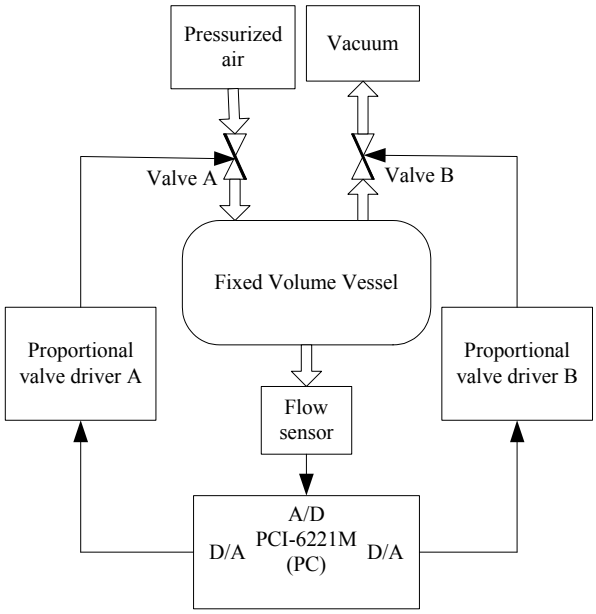

Fig. 10. Block diagram implementation of flow track design. Solid arrow lines illustrate electrical signal, hollow arrow lines illustrate airflow

A flow sensor (Honeywell, AWM5104) that outputs an analogue signal proportionally scaled to the applied flow was used to sample the flow of mouth. The analogue flow signal is conditioned and low-pass filtered using a 2nd-order digital Butterworth filter with a 50 Hz cutoff frequency to remove high-frequency noise due to turbulent flow inside the FVV. The analogue flow pressure signal was sampled with a 16-bit ADC, i.e., analog input in PCI-6221M.

There are many methods for the PID adjusting. The PID parameters were selected based on the extended step response curve methods. The steps for the PID parameters adjustment were as following:

1. digital controller does not worked in system, the process variable of controlling object was adjusted to the values near setpoint. The variable values were stabilized, and then unit step response curve was measured.
2. a tangent at inflexion in response curve is located. Delayed time τ and time constant T_m and ratio of the two parameters T_m/τ were calculated.
3. controlling degree was selected.
4. parameters T, K_p, T_i and T_d were calculated based on table (Gao, 2007).

The final parameters we selected were listed: P=3, I=0.8, D=0. The controller can be more efficient if adaptive-tuning scheme based on adaptive signal processing techniques was implemented to tune automatically.

Tracking result was shown in figure 11. It can be concluded that in the normal breath pattern the practical flow was very much alike to the theoretical flow curve. More details are to be exploited in future. And more pathology breath options should be studied to get a more complicated understanding to the flow tracking method.

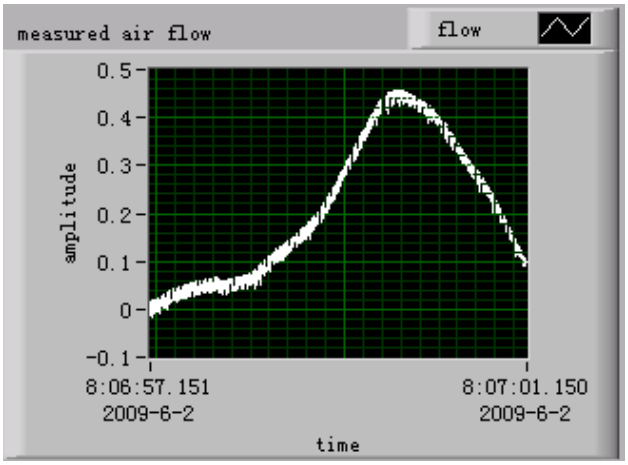

Fig. 11. Measured flow waveform by flow tracking algorithm using PID, which is very similar to the calculated wave.

6.4 Simulation of spontaneous respiration nonlinear model

There are two methods that we can use to simulate the respiratory system. First, simulink toolkits in matlab are the commonly used tool for simulation. But the simulink can not interface control system real-time, although it is powerful in model simulation. Second, the control design and simulation module in LabVIEW can also be used. On advantage of LabVIEW's interface convenience, the model design by control design and simulation module can be used in real actuator control very easy. But the disadvantage of the module is it can not design model by block. If the model is somewhat complicate, the control design and simulation module will become powerless. Fortunately, the National Instruments Company realize the problem, they provide a tool, i.e., simulation interface toolkits, used to transform Simulink model to LabVIEW program. Combine the advantage of powerful model construction of simulink and interface convenience with peripheral actuator of LabVIEW and the bridge tool simulation interface toolkits (SIT), we design a program based on LabVIEW with SIT interface with simulation model generated by simulink. The program can control actuator and designs the simulation model complicate, which take advantage while eliminate disadvantage of the two languages.

The equation of motion that represents the nonlinear model is (Jandre, 2005):

$$P = \left(K_1 + K_2 \left|\dot{V}(t)\right|\right)\dot{V}(t) + E \cdot V(t) \tag{19}$$

The respiratory muscle pressure data from Jodat (1966) is used as input of model. We construct the nonlinear model of breath system using simulink, the following block in Fig. 12 being the model, parameters were selected from Tang (1995). The LabVIEW 8.6 and SIT 5.0 is used in the main program, DAQ is configured to output signal with PCI-6221M card equipped. The calculated flow wave is to be tracked by proportional flow valve. Fig.13 is part of front panel when SIT is used interface with simulink. Fig.14 is the simulated flow using the aforementioned simulation condition: respiratory muscle used as input, nonlinear parameter of resistance that flow-dependent is used, and compliance is fix number.

Compared with the flow wave generated with fixed resistance (He, 2009(b)), the inspiratory flow part has little change, but the expiratory flow parts are smoother. In general, the flow is more similar to the real curve. We have tried the two foregoing methods both respectively (He, 2009(a, b)). But we can not realize the simulation construction and output simulated result by one program. If the model is simple, the control design and simulation module in LabVIEW can competent for the task, as we have done in previous work. With the complicate of respiratory model, by practice, we conclude that the combination of simulink and LabVIEW bridged by simulation interface toolkits is the optimum option.

There are three main key points in the chapter: (1) the respiratory muscle pressure is used as system input, which is accorded with spontaneous breath principle; (2) respiratory model is more complicated and precise with resistance flow-dependent parameterized, and the computed flow is even similar to real breath; (3) LabVIEW is used as the main program to interface with peripheral equipment, simulink is used as model construction program to cope with model complication, SIT is used to bridge the two program efficiently. The mentioned program method should be the optimum solution by our practice.

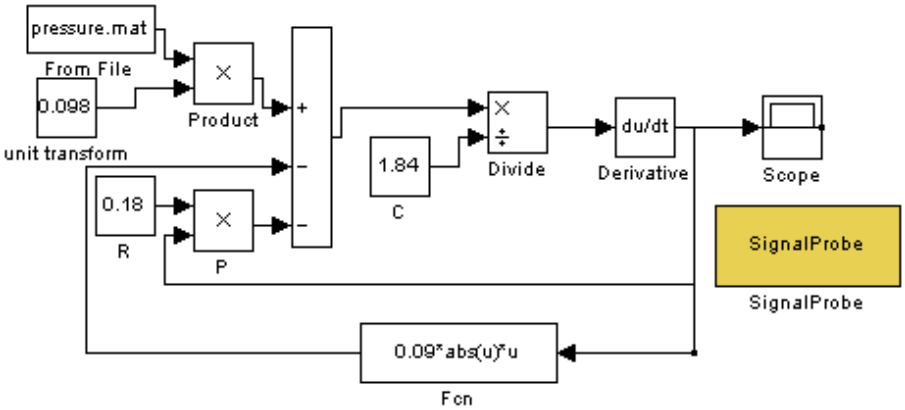

Fig. 12. Simulink model with muscle pressure as input and linear compliance nonlinear resistance varied with flow

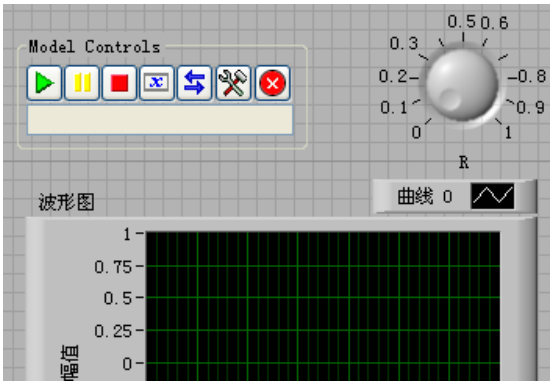

Fig. 13. Part of front panel of LabVIEW program when simulation interface toolkits are used to embed simulink mode

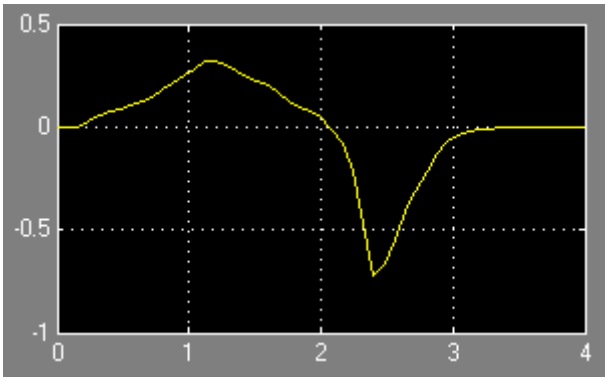

Fig.14. Simulation result of flow using muscle pressure as input and nonlinear airway resistance

7. Conclusion

In this chapter, respiratory model is studies including simple model and complicated nonlinear model. The realize method is introduced that have can control output flow. Two main simulate way, i.e., simulink and LabVIEW, are used to model the respiratory movement. The combined method that can integrate the advantage of the two method is illustrated for control aim. In general, this chapter provide a through introduction for respiratory modelling and control design.

8. References

Bachy, Jean-pierre, Eberhard, A., Baconnier, P. and Benchetrit, G. (1986). A program for cycle-by-cycle shape analysis of biological rhythms. Application to respiratory rhythm. Computer methods and programs in biomedicine, Vol. 23, 297-307.

Ball, W. C. (1996). Interactive respiratory physiology, John Hopkins School of Medicine, http://oac.med.jhmi.edu/res_phys/Encyclopedia/AirwayResistance/AirwayResistance.HTML

Barkalow, C. E., Morsley, K. C., (1974). Pneumatic lung analog. US Patent, 3808706.

Barkalow (1984). Pneumatic lung analog for simulation of spontaneous breathing and for testing of ventilatory devices used with spontaneously breathing patients. US Patent, 4430893.

Bayliss, L. and Robertson, G. (1939). The visco-elastic properties of the lungs. Quarterly journal of experimental physiology. Vol. 29, 27-47.

Benchetrit, G. (2000). Breathing pattern in humans: diversity and individuality. Respiration physiology, Vol. 122, 124-129.

Bertram, C.D. (1995). The dynamics of collapsible tubes. In: Ellington, C.P., Pedley, T.J. (Eds.), Biological fluid dynamics, 253-264.

Gao, Jinyuan, Xia, Jie (2007). Computer control systems. Tsinghua university press, Beijing.

Grinnan, D. C. and Truwit, J. D. (2005). Clinical review: Respiratory mechanics in spontaneous and assisted ventilation. Critical Care, Vol. 9, No.5, 472-484.

Guyton, Authur C., Hall, John E. (2002). Textbook of medical physiology (tenth edition). Beijing medical university press, Beijing.

He, Zhonghai (2009, a). Simulation study on human respiratory system based on muscle pressure driven. International conference on engineering computation. Hong Kong: IEEE computer society, 33-35.

He, Zhonghai, Shan, Fang, Sun, Meirong (2009, b). Adjustable parameters respiratory flow generation simulation method realized by LabVIEW. Third international symposium on intelligent information technology application, Nanchang, IEEE computer society, 299-301.

Jandre, F. C., Carvalho, A. R. S., Pino, A. V., Antonio G. (2005). Effects of filtering and delays on the estimates of a nonlinear respiratory mechanics model. Respiratory Physiology & Neurobiology, Vol. 148, 309–314.

Jandre, F., Pino, A., Lacorte, I., Soares, J., Giannella-Neto, A. (2004). A closed-loop mechanical ventilation controller with explicit objective functions. IEEE transactions on biomedical engineering, Vol. 51, 823-831.

Jansen, J. R. C., Hoorn, E., Goudoever, J., and Versprille, A. (1989). A computerized respiratory system including test functions of lung and circulation. Journal of applied physiology, Vol. 67, No. 4, 1687-1691.

Jodat, R. W., Horgen, J. D., and Lange, R. L. (1966). Simulation of respiratory mechanics. Biophysical journal, Vol. 6, 773-785.

Lambert, R. K., Wilson, T. A., Hyatt, R. E., and Rodarte, J. R. (1982). A computational model for expiratory flow. Journal of applied physiology, Vol. 52, No. 1, 44-56.

Ma, Dayou, Shen, Hao (1983). Acoustics handbook. Beijing, China: Science press.

Mauroy, B., Filoche, M., Weibel, E. R., Sapoval, B. (2004). An optimal bronchial tree may be dangerous. Nature, Vol. 427, 633-636.

Mecklenburgh, J. S. (1988). Construction of linear resistance units for a model lung. Medical & Biological Engineering & Computing, Vol. 26, 552-554.

Meka, V. V., van Oostrom, J. H. (2004). Bellow-less lung system for the human patient simulator. Medical & Biological engineering & computing, Vol. 42, 413-418.

Meyer, M. (1983). A versatile hydraulically operated respiratory servo system for ventilation and lung function testing. Journal of applied physiology, Vol.55, 1023-1030.

Myojo, T. (1989). Breathing pattern simulation using slit/cam valve. American industrial hygiene association journal, Vol.50, No.5, 240-244.

Otis, Arthur B., McKerrow, Colin B., Bartlett, Richard A., Mead, Jere et al. (1956). Mechanical factors in distribution of pulmonary ventilation. Journal of applied physiology, Vol.8, No. 4, 427-443.

Polak, Adam G. (1998). A forward model for maximum expiration [J]. Computers in biology and medicine, Vol.28, 613-625.

Polak, Adam G. (2003). Computational model for forced expiration from asymmetric normal lungs. Annals of biomedical engineering, Vol. 31, 891-907.

Polak, Adam G., Mroczka, J. (2006). Nonlinear model for mechanical ventilation of human lungs. Computers in biology and medicine, Vol. 36, 41-58.

Polak, Adam G.. (2008). A model-based method for limitation analysis in the heterogeneous human lung. Computer methods and programs in biomedicine, Vol. 89, 123-131.

Quatember, B. (2003). Human respiratory system: simulation of breathing mechanics and gas mixing processes based on a non-linear mathematical model. International

conference on health sciences simulation, University of Innsbruck, Innsbruck, Austria.

Renolds, D.B. (1982). Steady expiratory flow-pressure relationship of a model of the human bronchial tree, Journal of biomechanical engineering , Vol. 104, 153-158.

Rohrer F (1915). Flow resistance in human air passages and the effect of irregular branching of the bronchial system on the respiratory process in various regions of the lungs. Arch. Ges. Physiol, Vol. 162, 225-229.

Tang Yuansheng, Zhang Xiuzhen, Han diancun (1995). Parameters and concept of human medical. Jinan publishing house, Jinan.

Tantucci, C., Duguet, A., Giampiccolo, P., Similowski, T., Zelter, M., Derenne, J.P. (2002). The best peak expiratory flow is flow-limited and effort-independent in normal subjects. American journal of respiratory critical care medicine, Vol. 165, 1304-1308.

Verbraak, A. F. M., Bogaard, J. M., Beneken, J. E. W., Hoorn, E., Versprille, A. (1991). Serial lung model for simulation and parameter estimation in body plethysmography. Medical & biological engineering & computing, Vol. 29, 309-317.

Verbraak, A. F. M., Rijnbeek, P. R., Beneken, J. E. W., Bogaard, J. M., Versprille, A. (1995). Computer-controlled mechanical lung model for application in pulmonary function studies. Medical & biological engineering & computing, Vol. 33, 776-783.

Verbraak, A. F. M., Rijnbeek, P. R., Beneken, J. E. W., Bogaard, J. M., Versprille, A. (2001). A new approach to mechanical simulation of lung behaviour: pressure-controlled and time-related piston movement. Medical & biological engineering & computing, Vol. 39, 82-89.

Verbraak, A F. M., Mesic, S., Babuska, R., Hoogsteden, H. C. (2003). Computer-controlled mechanical simulation of the artificially ventilated human respiratory system. IEEE transactions on biomedical engineering, Vol. 50, No. 6, 731-743.

Weibel, E. R. (1963). Morphometry of the human lung. Springer-Verlag, Berlin.

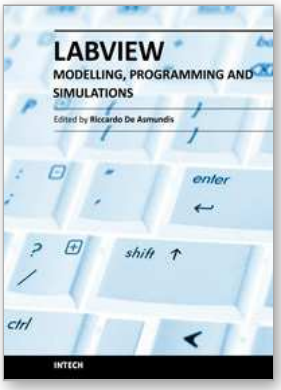

Modeling, Programming and Simulations Using LabVIEW™ Software

Edited by Dr Riccardo De Asmundis

ISBN 978-953-307-521-1
Hard cover, 306 pages
Publisher InTech
Published online 21, January, 2011
Published in print edition January, 2011

Born originally as a software for instrumentation control, LabVIEW became quickly a very powerful programming language, having some characteristics which made it unique: simplicity in creating very effective User Interfaces and the G programming mode. While the former allows for the design of very professional control panels and whole applications, complete with features for distributing and installing them, the latter represents an innovative way of programming: the graphical representation of the code. The surprising aspect is that such a way of conceiving algorithms is extremely similar to the SADT method (Structured Analysis and Design Technique) introduced by Douglas T. Ross and SofTech, Inc. (USA) in 1969 from an original idea by MIT, and extensively used by the US Air Force for their projects. LabVIEW enables programming by implementing directly the equivalent of an SADT "actigram". Apart from this academic aspect, LabVIEW can be used in a variety of forms, creating projects that can spread over an enormous field of applications: from control and monitoring software to data treatment and archiving; from modeling to instrument control; from real time programming to advanced analysis tools with very powerful mathematical algorithms ready to use; from full integration with native hardware (by National Instruments) to an easy implementation of drivers for third party hardware. In this book a collection of applications covering a wide range of possibilities is presented. We go from simple or distributed control software to modeling done in LabVIEW; from very specific applications to usage in the educational environment.

How to reference

In order to correctly reference this scholarly work, feel free to copy and paste the following:

Zhonghai He and Yuqian Zhao (2011). Modeling in Respiratory Movement Using LabVIEW and Simulink, Modeling, Programming and Simulations Using LabVIEW™ Software, Dr Riccardo De Asmundis (Ed.), ISBN: 978-953-307-521-1, InTech, Available from: http://www.intechopen.com/books/modeling-programming-and-simulations-using-labview-software/modeling-in-respiratory-movement-using-labview-and-simulink

INTECH
open science | open minds

InTech Europe
University Campus STeP Ri
Slavka Krautzeka 83/A
51000 Rijeka, Croatia
Phone: +385 (51) 770 447

InTech China
Unit 405, Office Block, Hotel Equatorial Shanghai
No.65, Yan An Road (West), Shanghai, 200040, China
中国上海市延安西路65号上海国际贵都大饭店办公楼405单元
Phone: +86-21-62489820

Fax: +385 (51) 686 166
www.intechopen.com

Fax: +86-21-62489821